



# Eddy current technique as a nondestructive method for evaluating the degree of sensitization of 304 stainless steel

Yeganeh Kelidari<sup>a</sup>, Mehrdad Kashеfi<sup>a,\*</sup>, Mostafa Mirjalili<sup>a</sup>, Mahla Seyedi<sup>b</sup>, Thomas W. Krause<sup>c</sup>

<sup>a</sup> Department of Materials and Metallurgical Engineering, Faculty of Engineering, Ferdowsi University of Mashhad, Mashhad, Iran

<sup>b</sup> Corrosion and Metallurgy Study Centre "A. Daccò", University of Ferrara, Department of Engineering, via Saragat 4a, Ferrara, Italy

<sup>c</sup> Department of Physics and Space Science, Royal Military College of Canada, Kingston, ON, Canada, K7K 7B4

## ARTICLE INFO

### Keywords:

Degree of sensitization (DOS)  
Eddy current technique (ECT)  
Electrochemical potentiodynamic reactivation (DL-EPR)  
Intergranular corrosion (IGC)  
Stainless steel

## ABSTRACT

The application of eddy current (EC) technique in detection of sensitization before the occurrence of intergranular corrosion was investigated. For this purpose, EC experiments were performed on 304 stainless-steels sensitized at 650 °C and 750 °C for 1–20 hours. The double-loop electrochemical potentiodynamic reactivation (DL-EPR) and microstructural investigations were also carried out to evaluate the degree of sensitization (DOS). The DL-EPR results showed that the maximum sensitivity occurred within 4 h at 650 °C. The EC results indicated a reduction in voltage and impedance with increasing DOS. Finally, empirical relationships between DL-EPR and EC test results were developed.

## 1. Introduction

Austenitic stainless steels are among the most important engineering materials that are mainly used for their superior corrosion resistance. However, one of the main drawbacks of austenitic stainless steel is their sensitization during fabrication or heat treatment leading to corrosion at the grain boundaries when they are exposed to corrosive environments. In the other words, the sensitization decreases the steel's resistance to intergranular corrosion (IGC) and intergranular stress corrosion cracking (IGSCC) [1–4]. The sensitization of austenitic stainless steel occurs as a result of extreme heating or slow cooling from 850 to 450 °C. During sensitization, the chromium-rich carbides are deposited at the grain boundaries and chromium depletion of the area around the grain boundaries occurs [5–7].

The chromium depleted zones, adjacent to the grain boundaries, are more susceptible to corrosion due to their lower passivation capability. Therefore, by exposing the sensitized austenitic stainless steel to a corrosive environment, the chromium depleted zones are corroded and hence the intergranular corrosion occurs [8,9]. At high temperatures, the chromium diffusion from the matrix to the chromium depleted zone can be replenished. This is called "desensitization" or "healing" [8,10].

In austenitic stainless steels,  $M_{23}C_6$  carbide is the sensitizing agent. The amount of chromium in the chromium rich phases of  $M_{23}C_6$  carbides, are 2–4 times greater than the amount of chromium in the matrix. Consequently, the area surrounding the carbide precipitates are

depleted of chromium [8].

Sensitization of austenitic stainless steels is influenced by various factors such as chemical composition, deformation by cold work, grain-size, the fraction of martensite and ferrite, heating and cooling rate and heat treatment. The carbon and chromium content are the most important parameters controlling susceptibility of stainless steel to sensitization. Resistance to sensitization will improve by reducing the amount of carbon and increasing the chromium content in the stainless steels [9,11–17].

Various techniques are utilized to evaluate the susceptibility to sensitization and corrosion resistance of stainless steels [18]. The most common one is Electrochemical Potentiodynamic Reactivation (EPR) technique which is a destructive, quantitative and fast method and has been extensively used in the literature [19–23]. The ASTM A262: A-F standard [24] is normally used to quantify the degree of sensitization (DOS) of 304 and 304 L stainless steels [25].

In the DL-EPR technique, the specimen is polarized anodically from the open circuit potential (OCP), which is about  $-400$  mV/SCE up to  $+300$  mV/SCE and then reversed to the initial potential with the scanning rate of 6 mV/h [26]. The maximum current is measured in each loop. Finally, DOS values can be calculated using the ratio of maximum reactivation current density ( $I_r$ ) to the maximum activation current density ( $I_a$ ), using the following equation [26]:

$$\%DOS = \frac{I_r}{I_a} \times 100 \quad (1)$$

\* Corresponding author at: Ferdowsi University of Mashhad, Azadi Square, Mashhad, Razavi Khorasan, Iran.

E-mail address: [m-kashefi@ferdowsi.um.ac.ir](mailto:m-kashefi@ferdowsi.um.ac.ir) (M. Kashеfi).

<https://doi.org/10.1016/j.corsci.2020.108742>

Received 10 June 2019; Received in revised form 31 March 2020; Accepted 9 May 2020

Available online 18 May 2020

0010-938X/ © 2020 Elsevier Ltd. All rights reserved.

In recent years, the non-destructive evaluation of corrosion and sensitization in metals has been considered by many researchers [27,28]. One of the most common methods for non-destructive evaluation used in many recent evaluations [29] is eddy current technique, which is based on the principles of electromagnetic induction. To measure the eddy current outputs, a coil is placed on a conductive surface. Applying alternating sinusoidal current through the coil results in an alternating primary magnetic field. This primary field, in turn, induces eddy currents in the conductive material, which the coil is placed on. Consequently, a secondary magnetic field is produced by the eddy current that opposes the primary field (according to Lenz's law). The secondary magnetic field causes a change in the coil impedance [30].

One way to present eddy current results is by calculating the coil impedance ( $Z$ ). The impedance is the total resistance of the coil against the current and consists of two components; ohmic resistance ( $R$ ) and reactance ( $X$ ). The first component depends mainly on the electrical conductivity of the material, while the latter represents the inductive resistance against the coil current and are out of phase. The impedance and reactance values can be determined using Eqs. 2 and 3, respectively [31,32]:

$$Z = \frac{V}{I} = \sqrt{X^2 + R^2} \quad (2)$$

$$X = 2\pi fL = \frac{2\pi f\mu N^2 A}{l} \quad (3)$$

where  $\mu$ ,  $N$ ,  $A$ ,  $l$  and  $f$  are the magnetic permeability, number of coil turns, surface area of the coil, coil length, and the frequency of the primary field, respectively [31]. Change in the coil parameters affect eddy current outputs and subsequently makes changes in the impedance value.

The present study aims to investigate the applicability of non-destructive eddy current method in determining the occurrence as well as the degree of sensitization in the austenitic stainless steel. Utilizing this technique in measuring the EC voltage and impedance, a relation between EC response and the degree of sensitization was developed and a quick safety decision was made with no need for timely destructive sample preparation procedure.

## 2. Experimental procedure

### 2.1. Materials

304 austenitic stainless steel with chemical composition given in Table 1 was used in the present research.

304 austenitic stainless steel plates of  $6 \times 7 \text{ cm}^2$  and 3 mm thickness were solution annealed at  $1065 \text{ }^\circ\text{C}$  for 1 h followed by water quenching. Then, samples were sensitized by subjecting to various heat treatments at 650 and  $750 \text{ }^\circ\text{C}$  for different periods of time (1, 2, 4, 6, 10 and 20 h). Finally, the samples were air cooled.

### 2.2. Electrochemical techniques

The electrochemical techniques were conducted using a Gill AC automated potentiostat (ACM instruments). The measurements were carried out in the conventional three-electrode cell consisting of a saturated calomel electrode (SCE) as the reference electrode, a platinum foil as the counter electrode and a working electrode. The working

**Table 1**

Chemical composition of samples (304 austenitic stainless steel).

	C	Mn	P	S	Si	Cr	Ni	N	Fe
standard	0.08	2.00	0.045	0.030	1	18–20	8–12	0.10	Bal.
sample	0.056	0.76	0.025	0.012	0.41	18.13	8.25	0.048	Bal.

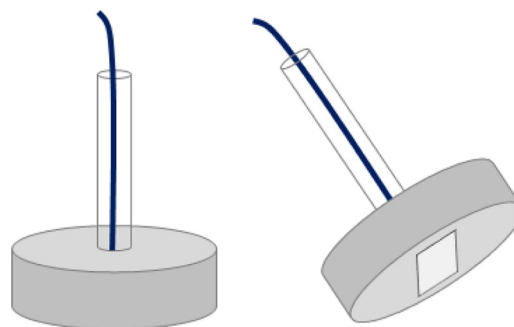


**Fig. 1.** Schematic of samples prepared for DL-EPR test.

electrode with the dimensions of  $1 \times 1 \times 0.3 \text{ cm}^3$  was mounted in a self-cured epoxy resin to offer an exposed surface area of  $1 \text{ cm}^2$ . The electrical contacts were connected by a screw at the back of the specimen, which was sealed using a long plastic tube (Fig. 1). Specimen surfaces were polished with 60–1200 grit grinding paper, washed thoroughly with distilled water, degreased in ethanol, dried with hot air and finally subjected to the test solution. All solutions were freshly prepared from analytical grade chemicals and distilled water. The electrolyte was composed of  $0.5 \text{ M H}_2\text{SO}_4 + 0.01 \text{ M}$  potassium thiocyanate (KSCN) solution.

The electrochemical cell was a 250 mL open beaker filled with 100 mL of the test solution. The intergranular corrosion resistance and the degree of sensitization (DOS) due to the different tempering conditions were investigated by double-loop electrochemical potentiodynamic tests (DL-EPR) [21]. Each DL-EPR polarization test was initiated by immersing the samples into the solution for 600 s until a steady state condition was reached (defined by a change of open circuit potential (OCP) of  $< 1 \text{ mV/min}$ ), followed by a potential sweep in the anodic direction from OCP up to  $450 \text{ mV/SCE}$  and then reversed to the initial potential with a scan rate of  $100 \text{ mV/min}$ . The DOS values were calculated using Eq. 1. Here,  $I_a$  is the peak current density during the forward (activation) scan and  $I_r$  is the peak current in the reversed (reactivation) scan. The DL-EPR tests were repeated 3 times for each sample to ensure their repeatability. The lower the  $I_r/I_a$  ratio, the lower the sensitization which has occurred in the specimen.

### 2.3. Microstructural examination

The microstructures were characterized using optical microscopy (OM). Corrosion of grain boundaries was revealed by electrolytic etching at 10 wt% aqueous solution of oxalic acid under a current density of  $1 \text{ A/cm}^2$  for 90 s according to ASTM A 262-91 Practice A [24]. Before electrochemical etching, the surface of the specimen was polished by  $0.05 \text{ }\mu\text{m}$  alumina slurry.

### 2.4. Eddy current testing (ECT)

The measurements were made on specimens with different aging temperatures. The eddy current tests were performed using a tailor-made instrument with a surface absolute probe of 5 mm diameter. The characteristics of primary (motivation) and secondary coils are listed in

**Table 2**

Characteristics of primary and secondary coils for eddy current test.

Parameters	Primary coil	Secondary coil
Number of the coil rounds	180	500
Insulated copper wire diameter	0.3 mm	0.2 mm
Height	5.5 mm	5.5 mm
Inner radius	11.8 mm	3.5 mm
Outer radius	15 mm	7.5 mm

**Table 2.** The secondary coil was designed to be surrounded by the primary coil (reflection probe with air core).

In this research, a function generator (Model AFG-500D, in the frequency range of 0.5 Hz to 50 kHz and 12 V peak to peak output voltages) was utilized for generating sinusoidal waves. The analog output from the probe was converted into a digital signal using a two channels oscilloscope and then the data were stored on a computer for analysis. The ECT lift-off (distance between the specimen and the ECT probe) was considered to be constant (ECT probe was in contact with the specimen). Each EC response, was repeated 5 times at different locations of the specimen surface and the averaged data was reported for each measurement.

### 2.5. Measurement of electrical resistance and magnetic permeability

The electrical resistance of the metallic samples was measured by the four-point probe technique. In this method, four probes were placed on the sample at distances of 2 mm from each other. The voltage of 1 mV to 10 V was applied to the sample and the current was measured in the range of 0–200 mA. Finally, the electrical resistance of the sample was easily calculated.

The relative permeability of the samples was measured by LCR meter model GPS-3131B which permits measurement of relative magnetic permeability of steel samples.

## 3. Results and discussion

### 3.1. Measurement of degree of sensitization (DOS) using DL-EPR method

The assessment of the degree of the sensitization was carried out by the DL-EPR technique. The potential was swept from open circuit potential (OCP) up to 450 mV/SCE and then reversed to the initial potential using scanning rate of 100 mV/min. Fig. 2 shows the DL-EPR curve of the as-annealed specimen without any sensitization treatment (reference sample). Figs. 3 and 4 indicate the DL-EPR curves of the samples sensitized at 650 and 750 °C, respectively.

As can be seen, the specimens indicate a sudden passivation in the forward polarization at potentials around -100 mV/SCE, accompanied by a drop in the current density. The presence of chromium in the stainless steel composition is the main reason for formation of the passive film and subsequent resistance to corrosion attack. The minimum required chromium content in austenitic stainless steels is in the range of 12–13 % Cr. The nucleation and growth of chromium carbides in the grain boundaries affect the composition in the vicinity of the grain boundaries and cause formation of Cr-depleted regions in these sites. When chromium content in the local depleted regions falls below 12 %, degradation of local passivity occurs and thence specimen is

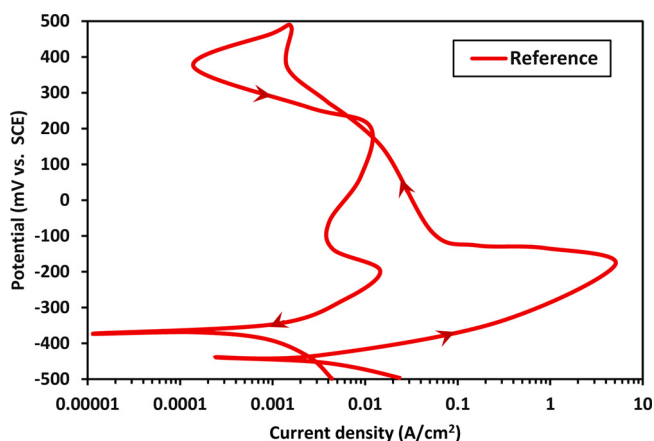


Fig. 2. DL-EPR curve for the specimen annealed at 1065 °C.

susceptible to intergranular corrosion or intergranular stress corrosion cracking [27,33,34]. Therefore, in the reverse polarization, the sensitized specimens have indicated higher current densities in comparison to the reference sample, especially higher reactivation peak current ( $I_r$ ) (Figs. 3 and 4). These higher current densities are a result of spreading Cr-depleted zones during aging and lower passivity of these regions [35]. It can be noticed that in the sensitized samples the maximum reactivation current density ( $I_r$ ) occurs at a more noble potential which means more susceptibility to corrosion [36].

The DOS values were calculated using the ratio of the reactivation current density ( $I_r$ ) to the activation current density ( $I_a$ ) in the DL-EPR curves (according to Eq. 1). The degree of sensitization for each of the samples is reported in Table 3. It can be concluded that for specimens that were heat treated at 650 and 750 °C, DOS values have increased by time. However, for longer heat treatment durations, the DOS value has decreased again. As indicated, the highest DOS value was obtained in the specimen tempered for 4 h. Increasing the aging time up to 10 h, has decreased the sensitization; so that no significant change at DOS has been observed by aging for 20 h. This phenomenon occurs as a result of chromium diffusion from the central areas of the grains to heal the Cr-depleted regions. It should be noted that aging temperature of 650 °C is not sufficient for complete desensitization of the specimen, even by prolonging the aging treatment to 20 h. It is reported that the recovery has not occurred even by 200 h aging at 650 °C [37].

By increasing the aging temperature to 750 °C, DOS has increased with time up to 4 h and then declined for further aging times. According to Cihal [38], by increasing the aging time, the chromium carbide and Cr-depleted regions increase due to a higher carbon diffusion coefficient compared with chromium. After reaching a critical aging time, the amount of carbon for diffusion decreases, but chromium diffuses continuously. Thus, the grain boundary Cr-depletion is self-healed by diffusion of chromium to the grain boundary area from the bulk of the austenite grains. According to Kina et al., aging at 750 °C for 48 h has resulted in complete desensitization [37].

Fig. 5 represents the relation between %DOS and aging time of the samples. According to Fig. 5 and Table 3, the maximum sensitization time is 4 h. The highest %DOS was obtained for the specimen aged at 650 °C, which is in agreement with previous studies [37].

### 3.2. Microstructural characterization

Fig. 6 shows the microstructure of samples after electrochemical etching in 10 % oxalic acid. Using electrochemical etching technique, the chromium carbides in the grain boundaries are dissolved causing ruggedness at grain boundaries. The first microstructure is a "step" structure seen in sensitized specimens with DOS lower than 4% (Fig. 6-a). This structure is observable when the carbides have not precipitated. A "dual" structure (Fig. 6-b) is seen in sensitized specimens with DOS ranging from 4 to 20 %. This structure is the result of discontinuous carbide precipitation. However, the "ditch" structure (Fig. 6-c and d) is observed in the sensitized specimens with DOS higher than 20 %. In this structure, a continuous carbide network is formed in the grain boundaries, which reveals a deep intergranular corrosion after etching (Fig. 6-d). This type of microstructure is characteristic of completely sensitized samples.

With regards to intergranular corrosion, the step and dual microstructures are acceptable, but the ditch structure is unwanted, as the corrosion attacks focus on the grain boundaries, due to the carbide precipitation in these regions [39]. Table 3 listed the DOS values and their related etching structures for each sample. In agreement with the DL-EPR results, samples aged at 750 °C, have indicated lower sensitization due to the healing effect.

### 3.3. Determining the degree of sensitization (DOS) by eddy current

When the eddy current probe is situated on the surface, eddy

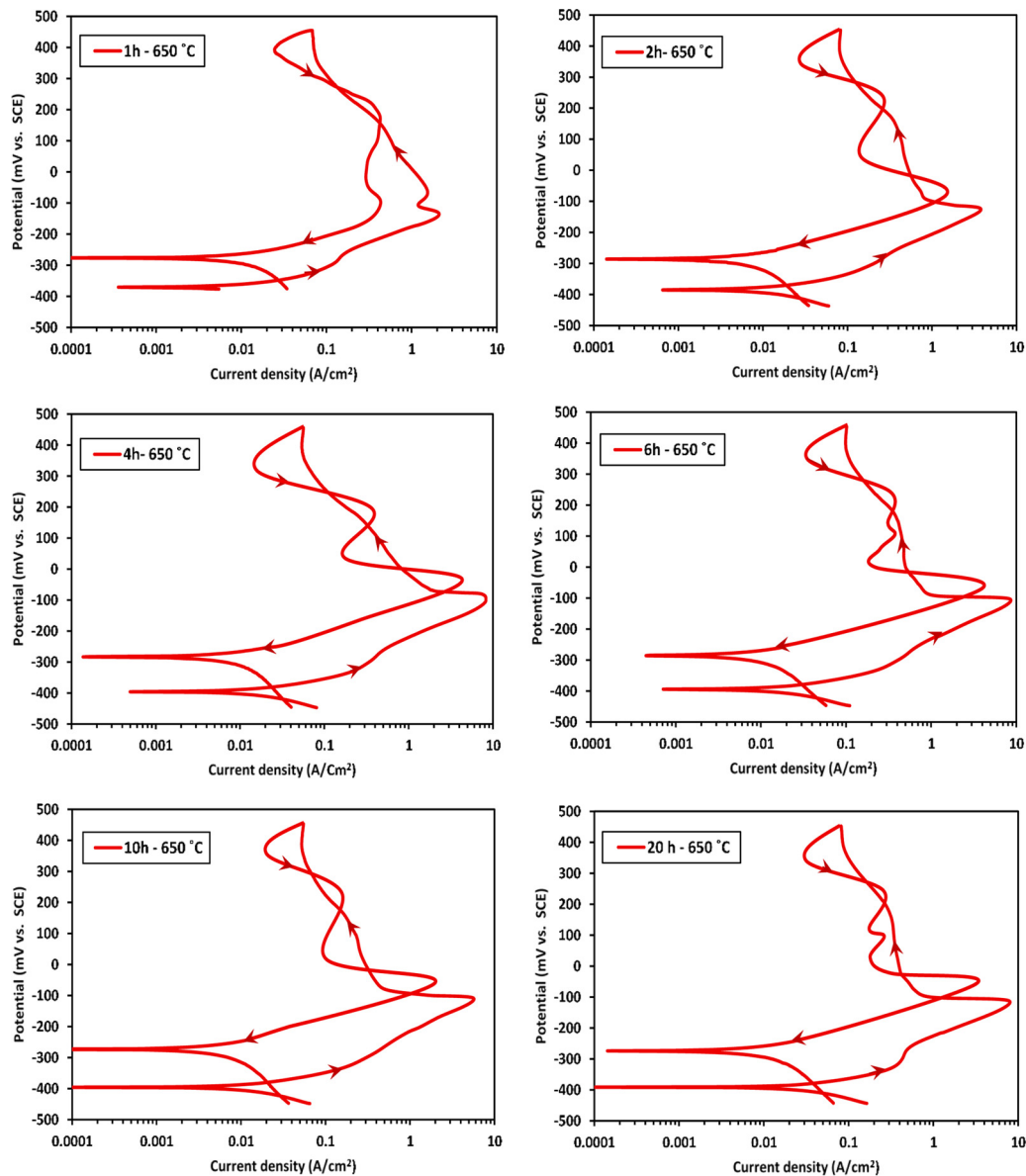


Fig. 3. DL-EPR curves for specimen which was sensitized at 650 °C for different periods of time.

currents are induced in the sample, which generate a secondary magnetic field in opposite direction. This opposite magnetic field interacts with the primary one causing measurable changes in overall magnetic field. Induced eddy current is a function of several electromagnetic parameters such as working frequency, electrical conductivity and magnetic permeability of the sample as well as some geometrical parameters such as lift-off, edge and skin effects. In the present research, the working frequency and geometrical parameters are set to be constant.

The first step in eddy current testing is determination of optimum frequency. In order to determine the optimum frequency, using the resolution method, the eddy current test response (voltage in this study) was measured for different samples in a range of frequencies. In this method, the optimum frequency [40] is the frequency at which the slightest change in conductivity or permeability of the material (caused by the sensitization) results in a maximum change in the voltage response.

For this purpose, three specimens were selected, two samples with 4 and 6 h aging at 750 °C (with low degrees of sensitization), as well as a third specimen with the highest degree of sensitization (4 h at 650 °C).

A range of frequencies were selected (10–600 kHz) and peak-to-peak voltage for all three specimens were obtained at the applied frequencies. As Fig. 7 shows, in the frequency range of 30–100 kHz (specially at 50 kHz), the eddy current test output indicates the highest difference between the specimens. Therefore, based on the resolution method, frequency of 50 kHz was chosen as the optimum frequency for obtaining the highest resolution of the voltage output of the eddy current tests. So that, this frequency was applied for the eddy current test of all samples.

Eddy current outputs at optimum frequency of 50 kHz are given in Table 4. As seen, by increasing the degree of sensitization (DOS), the response voltage of the eddy current test has decreased. This finding is in contrast to the previous results reported by Sheikh et al. [41,42]. They concluded that decreasing the level of chromium content at the grain boundaries (as a result of precipitation of chromium carbides) has led to an increase in the localized level of nickel content. Consequently, the Cr-depleted zones became more ferromagnetic resulting in higher magnetic permeability. In their idea, the magnetization of samples during the eddy current test was detected because of the change in magnetic permeability, which subsequently affected the output voltage

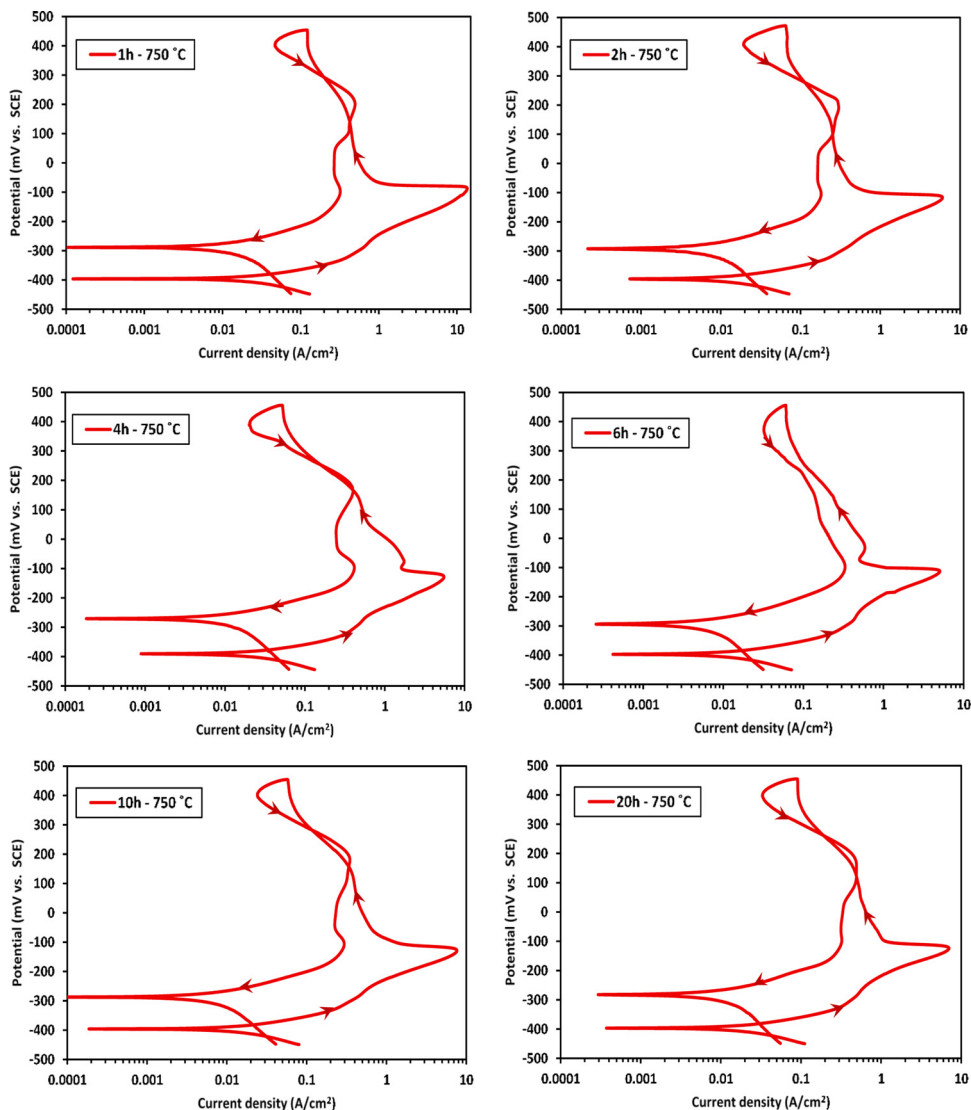


Fig. 4. DL-EPR curves for specimen which was sensitized at 750 °C for different periods of time.

**Table 3**  
Results of DL-EPR polarization and %DOS for 304 stainless steel.

Temperature	Time (hour)	%DOS Average	Standard deviation	Corroded structure
Ref (not sensitized)		0.32	0.096	Step structure
650 °C	1	20.37	1.005	Ditch structure
	2	35.88	0.661	Ditch structure
	4	47.93	1.477	Ditch structure
	6	44.85	1.694	Ditch structure
	10	38.91	1.100	Ditch structure
	20	40	1.165	Ditch structure
750 °C	1	3.66	0.401	Step structure
	2	4.98	0.255	Dual structure
	4	7.81	0.610	Dual structure
	6	6.32	0.760	Dual structure
	10	4.30	0.519	Dual structure
	20	6.76	0.617	Dual structure

of the test. However, it seems that etching the sample before eddy current test has a significant effect on their obtained results. The sensitized samples are more susceptible to corrosion especially at grain boundaries. When surface of a sensitized sample is etched, intergranular corrosion occurs resulting in formation of engraved boundaries (Fig. 7-d). As a result, surface conductivity decreases leading to

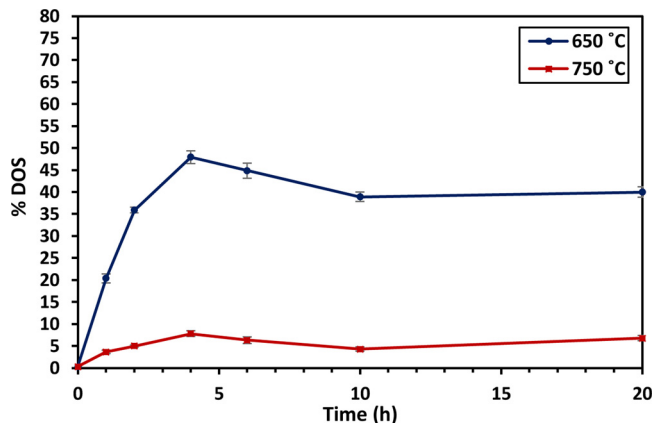
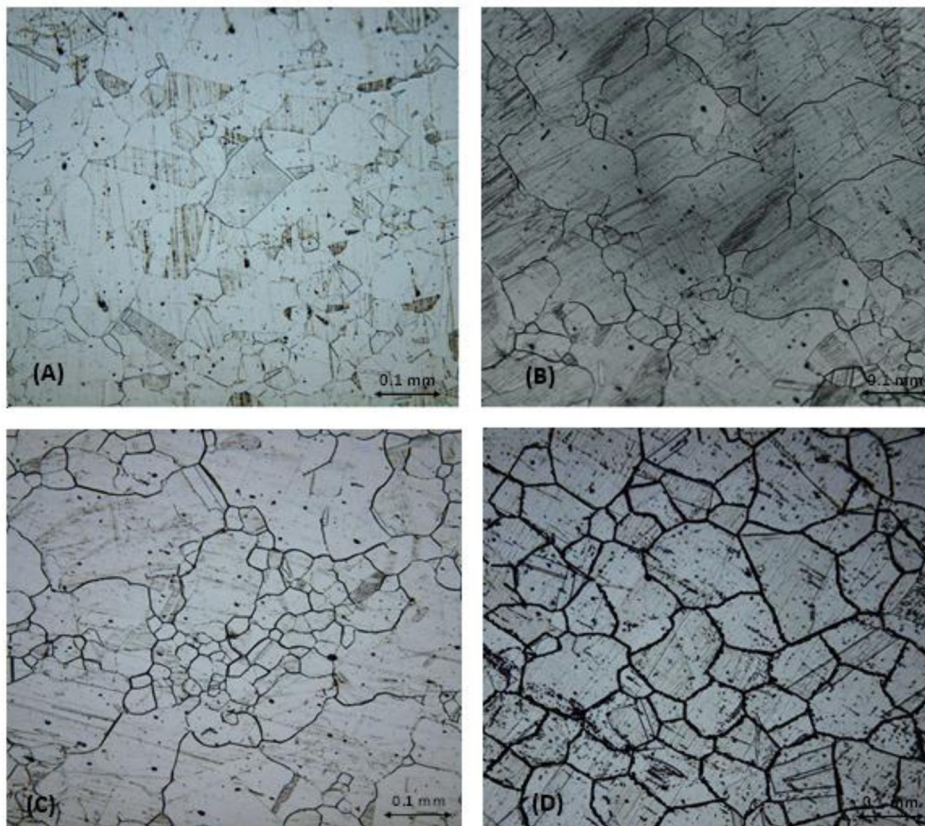


Fig. 5. The relation between %DOS and aging time for samples aged at 650 and 750 °C.

higher response voltage in sensitized samples. Therefore, the contradicting results obtained by Sheikh et al. [41,42] may be related to the surface preparation and etching in their work.

The results of relative permeability measurement are reported in Table 4. The relative permeability factor in all samples showed that



**Fig. 6.** Optical microscopic images of samples after electrochemical etching in 10 % oxalic acid: (a) step structure revealed in the reference sample (%0 sensitization) (b) dual structure revealed in the sample with %7.81 sensitization (c) ditch structure revealed in the sample with %20.37 sensitization and (d) ditch structure revealed in the sample with %40 sensitization.

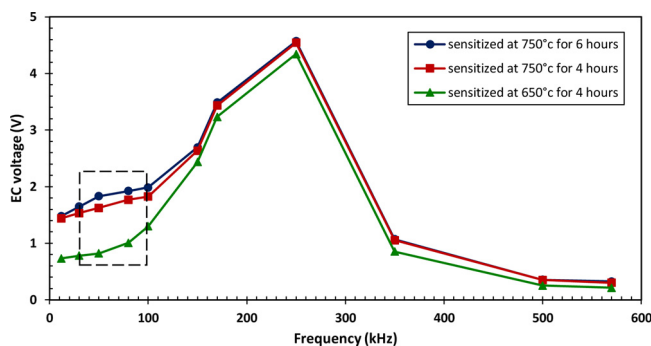


**Fig. 7.** Determination of optimum frequency based on the resolution method.

**Table 4**

Eddy current outputs and results of electrical resistance and relative permeability measurement for 304 stainless steel samples, which were sensitized at 650 and 750 °C.

Temperature	Time (h)	%DOS	EC voltage (mV)	STDEV for EC voltage	EC N. Impedance	STDEV for Impedance
650 °C	Ref sample	0.32	2165	8	1.020	0.008
	1	20.37	1316	16	0.860	0.018
	2	35.88	1132	9	0.800	0.009
	4	47.93	820	12	0.726	0.010
	6	44.85	912	7	0.749	0.008
	10	38.91	1084	11	0.781	0.008
750 °C	20	40	1022	7	0.770	0.005
	1	3.66	2045	12	0.982	0.005
	2	4.98	1924	21	0.966	0.007
	4	7.81	1626	8	0.922	0.008
	6	6.32	1830	14	0.941	0.012
	10	4.30	1987	18	0.973	0.008
	20	6.76	1792	11	0.935	0.010

magnetic permeability does not change considerably during sensitization. It is due to the non-magnetic nature of 304 stainless steel. Accordingly, the higher response voltage in sensitized samples in Sheikh et al. work, can be attributed to the surface etching. In contrast, samples in our experiments have not been etched, which is the innovation of our research and provides a means for non-destructive detection of the degree of sensitization in the austenitic stainless steels without the requirement of etching. As a result, the response voltage of the eddy current test in this non-destructive method decreases by the sensitization.

It should be considered that when a steel sample is sensitized, the matrix is relatively purified from its alloying elements (specially chromium) due to carbide formation, resulting in higher electrical conductivity and increasing the induced eddy current. This, in turn, alters the magnetic field in the secondary coil. Therefore, the peak-to-peak eddy current voltage decreases. To prove this claim, the electrical resistance of the samples was measured and reported in Table 4. As can be seen, the electrical resistance of the samples has decreased by increasing DOS.

The relation between DOS obtained by DL-EPR technique and the eddy current results is presented in Fig. 8. Accordingly, an experimental relation can be expressed in the following formula with a correlation coefficient ( $R^2$ ) of 0.9834.

$$\% \text{DOS} = 2 \times 10^{-5}(\text{EC Voltage})^2 - 0.1031 (\text{EC Voltage}) + 120.95 \quad (4)$$

This equation can be used to estimate the DOS according to the voltage of the eddy current test.

Another experimental feature which was used to investigate the sensitization of the specimens is impedance. The impedance ( $Z$ ) is a complex number and presents the resistance of a conductor component in the alternating current at a given frequency. The normalized impedance is derived from the division of impedance of each sample ( $Z$ ) to impedance of the empty coil ( $Z_0$ ). Fig. 9 depicts the normalized impedance versus %DOS. As illustrated, impedance decreases by %DOS,

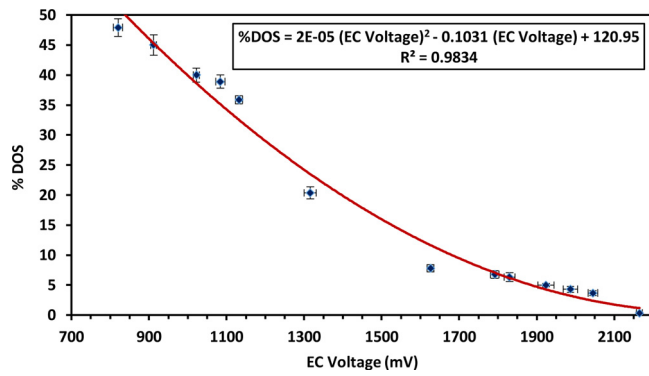


Fig. 8. The relation between %DOS measured by DL-EPR and EC voltage of the eddy current response.

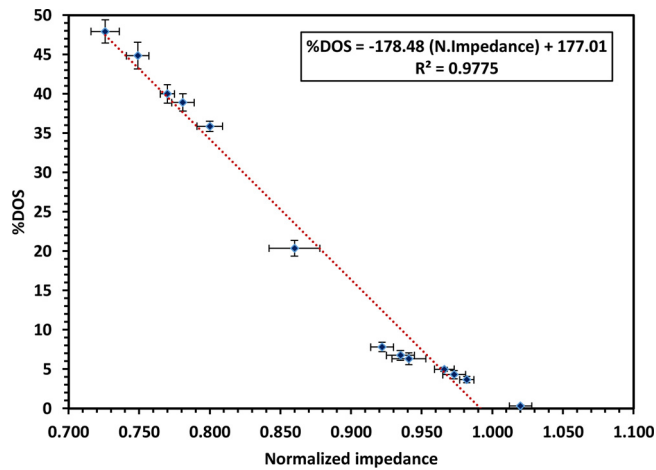


Fig. 9. The relation between %DOS measured by DL-EPR and normalized impedance.

according to following equation:

$$\%DOS = -178.48 (N. Impedance) + 177.01 \quad (5)$$

As mentioned previously, by increasing the degree of sensitization (DOS), the chromium content in the matrix decreases, which results in a reduction in electrical resistivity of the sample. Higher material conductivity generates more eddy currents providing a magnetic field in the same direction of that of the secondary coil. As a result, the measured impedance (Z) of the secondary coil will also decrease. This can be also understood from Eq. 2, which indicates that impedance (Z) decreases by decreasing resistance (R). Although in ferromagnetic materials permeability is the main factor [43], in non-magnetic austenitic 304 stainless steel electrical resistivity is the dominant one. Thus, by increasing the DOS, the measured impedance (Z) decreases.

As illustrated in Fig. 9, two different regions with distinct linear slopes are obvious: the region of low degrees of sensitization with %DOS values less than 10 %, and the region of high degrees of sensitization with %DOS values more than 10 %, respectively. Thus, for developing more precise equation between normalized impedance and %DOS, the graph was split into two regions as shown in Fig. 10-a and b. Fig. 10 depicts the extrapolation of the normalized impedance versus %DOS for the two above mentioned regions. Accordingly, two following equations are developed for low and high %DOS values, respectively:

$$\%DOS = -73.949 (N. Impedance) + 76.071 \quad (6)$$

$$\%DOS = -206.13 (N. impedance) + 198.98 \quad (7)$$

Considering that EC voltage and normalized impedance of the eddy current are used with no need for further sample preparation or

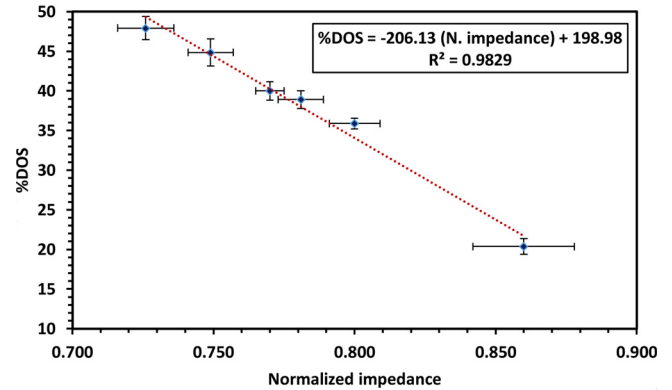
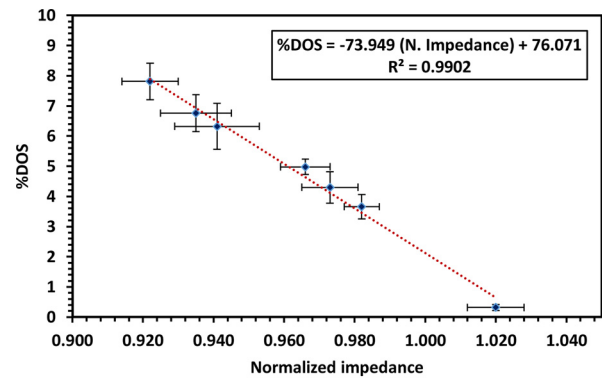


Fig. 10. The relation between %DOS measured by DL-EPR and normalized impedance in two regions of (a) low degrees of sensitization with %DOS values less than 10 %, and (b) high degrees of sensitization with %DOS values more than 10 %.

manipulation (etching) to estimate the degree of sensitization of stainless steels, the proposed non-destructive eddy current technique can be successfully used for inspection and detection of unexpected sensitization of stainless steel parts during the production process or service.

Finally, authors comment that if this non-destructive technique is to be used for estimating DOS, calibration is needed for each type of steel. For this purpose, first we need to sensitize samples of that type in such a way that different DOS values can be achieved from low to high. The DOS should be measured by conventional method such as DL-EPR, so the results can be used for finding a correlation between EC response and DOS.

#### 4. Conclusion

In the present study, DL-EPR and eddy current methods were utilized to determine the sensitization of 304 austenitic stainless steel. The main findings from this work are as follows:

- 1 Aging the specimens at 650 and 750 °C for 4 h has led to an increase in the degree of sensitization to 48 % and 8%, respectively. However, prolonging the aging time has caused lower sensitization due to healing effect.
- 2 Etching the sensitized specimen in oxalic acid has revealed that the sensitized specimens with %DOS lower than 4% exhibit the step structure, the sensitized specimens with %DOS in the range of 4–20 % indicate dual structure, and the sensitized specimens with %DOS greater than 20 % show ditch structure.
- 3 By increasing the DOS, both the normalized impedance and the response voltage of the eddy current test is reduced. Reduction of the impedance and voltage is attributed to increasing the electrical conductivity due to carbide precipitation and dilution of matrix.

4 The relationship between DL-EPR results and output voltage and impedance of the eddy current technique was established. The high correlation coefficients indicated that the outputs of the eddy current technique can be used precisely for non-destructive evaluation of degree of sensitization in the austenitic stainless steel parts.

### Author statements

Yeganeh Kelidari conceived the original idea, fabricated the sample, carried out the experiment with support from Mahla Seyedi, performed the analytic calculations and analysed the data, wrote the manuscript in consultation with Dr Thomas Krause. Dr Mehrdad Kashefi and Dr Mostafa Mirjalili supervised the project.

### Data availability

The raw/processed data required to reproduce these findings will be made available on request.

### CRedit authorship contribution statement

**Yeganeh Kelidari:** Conceptualization, Methodology, Formal analysis, Investigation, Resources, Writing - original draft, Visualization. **Mehrdad Kashefi:** Supervision. **Mostafa Mirjalili:** Supervision. **Mahla Seyedi:** Investigation. **Thomas W. Krause:** Writing - review & editing.

### Declaration of Competing Interest

There are no conflicts of interest.

### Acknowledgements

The authors are grateful to the financial support from Ferdowsi University of Mashhad provision of laboratory facilities during the period that this research was conducted.

### Appendix A. Supplementary data

Supplementary material related to this article can be found, in the online version, at doi:<https://doi.org/10.1016/j.corsci.2020.108742>.

### References

- S.K. B, B.S. Prasad, V. Kain, J. Reddy, Methods for making alloy 600 resistant to sensitization and intergranular corrosion, *Corros. Sci.* 70 (2013) 55–61, <https://doi.org/10.1016/j.corsci.2012.12.021>.
- B.Y. Fang, A. Atrens, J.Q. Wang, E.H. Han, Z.Y. Zhu, W. Ke, Review of stress corrosion cracking of pipeline steels in “low” and “high” pH solutions, *J. Mater. Sci.* 38 (2003) 127–132, <https://doi.org/10.1023/A:1021126202539>.
- E.A. Charles, R.N. Parkins, Generation of stress corrosion cracking environments at pipeline surfaces, *Corrosion* 51 (1995) 518–527, <https://doi.org/10.5006/1.3294372>.
- T. Fujii, K. Tohgo, Y. Mori, Y. Shimamura, Crystallography of intergranular corrosion in sensitized austenitic stainless steel, *Mater. Charact.* 144 (2018) 219–226, <https://doi.org/10.1016/j.matchar.2018.07.014>.
- M.A. Arafin, J.A. Szpunar, A new understanding of intergranular stress corrosion cracking resistance of pipeline steel through grain boundary character and crystallographic texture studies, *Corros. Sci.* 51 (2009) 119–128, <https://doi.org/10.1016/j.corsci.2008.10.006>.
- A. Abou-Elazm, R. Abdel-Karim, I. Elmahallawi, R. Rashad, Correlation between the degree of sensitization and stress corrosion cracking susceptibility of type 304H stainless steel, *Corros. Sci.* 51 (2009) 203–208, <https://doi.org/10.1016/j.corsci.2008.10.015>.
- K. Kaneko, T. Fukunaga, K. Yamada, N. Nakada, M. Kikuchi, Z. Saghii, J.S. Barnard, P.A. Midgley, Formation of M23C6-type precipitates and chromium-depleted zones in austenite stainless steel, *Scr. Mater.* 65 (2011) 509–512, <https://doi.org/10.1016/j.scriptamat.2011.06.010>.
- N. Parvathavarthini, Sensitization and testing for intergranular corrosion, *Corros. Austenitic Stainl. Steels.* (2002) 117–138, <https://doi.org/10.1533/9780857094018.139>.
- N. Parvathavarthini, R.K. Dayal, J.B. Gnanamoorthy, Influence of prior deformation on the sensitization of AISI Type 316LN stainless steel, *J. Nucl. Phys. Mater. Sci. Radiat. Appl.* 208 (1994) 251–258, [https://doi.org/10.1016/0022-3115\(94\)90334-4](https://doi.org/10.1016/0022-3115(94)90334-4).
- H.S. Khatak, B. Raj, *Corrosion of Austenitic Stainless Steels: Mechanism, Mitigation and Monitoring*, Elsevier Science, 2002.
- T.A. Mozhi, W.A.T. Clark, K. Nishimoto, W.B. Johnson, D.D. Macdonald, The Effect of Nitrogen on the Sensitization of AISI 304 Stainless Steel, *Corrosion* 41 (1985) 555–559, <https://doi.org/10.5006/1.3582983>.
- N. Parvathavarthini, R.K. Dayal, S.K. Seshadri, J.B. Gnanamoorthy, Continuous cooling and low temperature sensitization of AISI types 316 SS and 304 SS with different degrees of cold work, *J. Nucl. Phys. Mater. Sci. Radiat. Appl.* 168 (1989) 83–96, [https://doi.org/10.1016/0022-3115\(89\)90568-0](https://doi.org/10.1016/0022-3115(89)90568-0).
- H. Kokawa, M. Shimanda, Y.S. Sato, Alloy Science Research Summary, (2000), pp. 34–37 <https://link.springer-com.openathens-proxy.swan.ac.uk/content/pdf/10.1007/s11837-000-0159-0.pdf>.
- E.A. Trillo, L.E. Murr, Effects of carbon content, deformation, and interfacial energetics on carbide precipitation and corrosion sensitization in 304 stainless steel, *Acta Mater.* 47 (1998) 235–245, [https://doi.org/10.1016/S1359-6454\(98\)00322-X](https://doi.org/10.1016/S1359-6454(98)00322-X).
- N. Parvathavarthini, R.K. Dayal, Time-temperature-sensitization diagrams and critical cooling rates of different nitrogen containing austenitic stainless steels, *J. Nucl. Phys. Mater. Sci. Radiat. Appl.* 399 (2010) 62–67, <https://doi.org/10.1016/j.jnucmat.2010.01.003>.
- C. Garda, F. Martin, P. De Tiedra, J.A. Heredero, M.L. Aparicio, Effect of prior cold work on intergranular and transgranular corrosion in type 304 stainless steels: quantitative discrimination by image analysis, *Corrosion* 56 (2000) 243–255.
- R. Pascali, A. Benvenuti, D. Wenger, Carbon content and grain size effects on the sensitization of AISI type 304 stainless steels, *Corrosion* 40 (1984) 21–32, <https://doi.org/10.5006/1.3579291>.
- W. Stichel, *Corrosion Tests and Standards: Application and Interpretation*, Hrsg. R. Baboian, 764 Seiten, ASTM, Philadelphia, USA, 1995, <https://doi.org/10.1002/maco.19960470809> Pries £ 85.-, ISBN 0-8031-2058-3. In Europa erhältlich bei: American Technical Publishers Ltd, 27-29 Knowl Piece, Wilbury Way, Hitchin, Herts, SG4 0SX, England, Mater. Corros. Und Korrosion. 47 (1996) 461–461.
- G.H. Aydođdu, M.K. Aydinol, Determination of susceptibility to intergranular corrosion and electrochemical reactivation behaviour of AISI 316L type stainless steel, *Corros. Sci.* 48 (2006) 3565–3583, <https://doi.org/10.1016/j.corsci.2006.01.003>.
- S. Chen, H. Huang, C. Liu, Y. Pan, Technique for detecting sensitization in austenitic stainless steel, *Corrosion* 48 (1992) 594–598, <https://doi.org/10.5006/1.3315977>.
- N. Lopez, M. Cid, M. Puiggali, I. Azkarate, A. Pelayo, Application of double loop electrochemical potentiodynamic reactivation test to austenitic and duplex stainless steels, *Mater. Sci. Eng. A* 229 (1997) 123–128, [https://doi.org/10.1016/S0921-5093\(97\)00008-7](https://doi.org/10.1016/S0921-5093(97)00008-7).
- T.F. Wu, W.T. Tsai, Effect of KSCN and its concentration on the reactivation behavior of sensitized alloy 600 in sulfuric acid solution, *Corros. Sci.* 45 (2003) 267–280, [https://doi.org/10.1016/S0010-938X\(02\)00100-2](https://doi.org/10.1016/S0010-938X(02)00100-2).
- K.S. de Assis, F.V.V. de Sousa, M. Miranda, I.C.P. Margarit-Mattos, V. Vivier, O.R. Mattos, Assessment of electrochemical methods used on corrosion of superduplex stainless steel, *Corros. Sci.* 59 (2012) 71–80, <https://doi.org/10.1016/j.corsci.2012.02.014>.
- ASTM Norma, Standard Practices for Detecting Susceptibility to Intergranular Attack in Austenitic. A262, ASTM Copyright. 01, (2014), pp. 1–17, <https://doi.org/10.1520/A0262-13>.
- I. Astm, ASTM G108-94: standard test method for electrochemical reactivation (EPR) for detecting sensitization of AISI type 304 and 304L stainless steels, *Annu. Book ASTM Stand. Sect. Water Environ. Technol.* 94 (2010) 1–9, <https://doi.org/10.1520/G0108-94R10.2>.
- R. Baboian, *Corrosion Tests and Standards: Application and Interpretation*, ASTM, 1995, <https://books.google.it/books?id=8C7pXhnqje4C>.
- C. Doerr, J.Y. Kim, P. Singh, J.J. Wall, L.J. Jacobs, Evaluation of sensitization in stainless steel 304 and 304L using nonlinear Rayleigh waves, *NDT E Int.* 88 (2017) 17–23, <https://doi.org/10.1016/j.ndteint.2017.02.007>.
- J. Jingpin, S. Junjun, L. Guanghai, W. Bin, H. Cunfu, Evaluation of the intergranular corrosion in austenitic stainless steel using collinear wave mixing method, *NDT E Int.* 69 (2015) 1–8, <https://doi.org/10.1016/j.ndteint.2014.09.001>.
- O. Mareschal, C. Cordier, C. Dolabdjian, P. Finkel, Aluminum alloy sensitization evaluation by using eddy current techniques based on IGMR-magnetometer head, *IEEE Trans. Magn.* 55 (2019) 1–4, <https://doi.org/10.1109/TMAG.2018.2873211>.
- P.J. Shull, M. Dekker (Ed.), *Nondestructive Evaluation: Theory, Techniques, and Applications*, 2002 (Accessed 29 May 2019), <https://www.crcpress.com/Nondestructive-Evaluation-Theory-Techniques-and-Applications/Shull/p/book/9780824788728>.
- R. Meyendorf, *Nondestructive Determination of Case Depth in Surface Hardened Steels by Combination of Electromagnetic Test Methods*, (2011) (Accessed 29 May 2019), [https://etd.ohiolink.edu/pg\\_10?0:NO:10:P10\\_ETD\\_SUBID:53649](https://etd.ohiolink.edu/pg_10?0:NO:10:P10_ETD_SUBID:53649).
- S. Ghanei, M. Kashefi, M. Mazinani, Comparative study of eddy current and Barkhausen noise nondestructive testing methods in microstructural examination of ferrite-martensite dual-phase steel, *J. Magn. Magn. Mater.* 356 (2014) 103–110, <https://doi.org/10.1016/j.jmmm.2014.01.001>.
- C.O.A. Olsson, *Passivation of Stainless Steels and Other Chromium Bearing Alloys*, Elsevier, 2018, <https://doi.org/10.1016/b978-0-12-409547-2.13585-1>.
- N. Parvathavarthini, S. Mulki, R.K. Dayal, I. Samajdar, K.V. Mani, B. Raj, Sensitization control in AISI 316(LN) austenitic stainless steel: defining the role of the nature of grain boundary, *Corros. Sci.* 51 (2009) 2144–2150, <https://doi.org/10.1016/j.corsci.2009.05.045>.
- R. Wang, Z. Zheng, Q. Zhou, Y. Gao, Effect of surface nanocrystallization on the sensitization and desensitization behavior of Super304H stainless steel, *Corros. Sci.*

- 111 (2016) 728–741, <https://doi.org/10.1016/J.CORSCI.2016.06.012>.
- [36] R. Wang, Z. Zheng, Q. Zhou, Y. Gao, Effect of surface nanocrystallization on the sensitization and desensitization behavior of Super304H stainless steel, *Corros. Sci.* 111 (2016) 728–741, <https://doi.org/10.1016/j.corsci.2016.06.012>.
- [37] A.Y. Kina, V.M. Souza, S.S.M. Tavares, J.M. Pardal, J.A. Souza, Microstructure and intergranular corrosion resistance evaluation of AISI 304 steel for high temperature service, *Mater. Charact.* 59 (2008) 651–655, <https://doi.org/10.1016/j.matchar.2007.04.004>.
- [38] V. Číhal, *Intergranular Corrosion of Steels and Alloys*, Elsevier, 1984.
- [39] American Society for Testing and Materials, *Annual Book of ASTM Standards*, ASTM, 1970 (Accessed 29 May 2019), [https://trove.nla.gov.au/work/9568569?q&sort=holdings+desc&\\_id=1559115868050&versionId=22760498](https://trove.nla.gov.au/work/9568569?q&sort=holdings+desc&_id=1559115868050&versionId=22760498).
- [40] V.S. Cecco, G. Van Drunen, F.L. Sharp, *Eddy Current Manual Volume 1: Test Method*, (1981), p. 208 [http://www.iaea.org/inis/collection/NCLCollectionStore/\\_Public/15/061/15061786.pdf](http://www.iaea.org/inis/collection/NCLCollectionStore/_Public/15/061/15061786.pdf).
- [41] H. Shaikh, N. Sivaibharasi, B. Sasi, T. Anita, R. Amirthalingam, B.P.C. Rao, T. Jayakumar, H.S. Khatak, B. Raj, Use of eddy current testing method in detection and evaluation of sensitisation and intergranular corrosion in austenitic stainless steels, *Corros. Sci.* 48 (2006) 1462–1482, <https://doi.org/10.1016/j.corsci.2005.05.017>.
- [42] H. Shaikh, B.P.C. Rao, S. Gupta, R.P. George, S. Venugopal, B. Sasi, T. Jayakumar, H.S. Khatak, Assessment of intergranular corrosion in AISI Type 316L stainless steel weldments, *Br. Corros. J.* 37 (2002) 129–140, <https://doi.org/10.1179/000705902225004419>.
- [43] C. Moosbrugger, *ASM Ready Reference: Electrical and Magnetic Properties of Metals*, ASM International, 2000, <https://books.google.it/books?id=PZFmZNVV5TIC>.